Sustainable Cities and Society 132 (2025) 106804

Contents lists available at ScienceDirect

Sustainable Cities and Society

journal homepage: www.elsevier.com/locate/scs

Assessing urban emergency medical services accessibility for older adults considering ambulance trafficability using a deep learning approach

Zhuo Liu [a,b], Enjia Zhang [c,*], Shuo Pan [a], Sichun Li [a], Ying Long [d], Frank Witlox [b]

[a] Beijing Key Laboratory of Traffic Engineering, Beijing University of Technology, Beijing, China
[b] Department of Geography, Ghent University, Ghent, Belgium
[c] College of Architecture and Urban Planning, Beijing University of Technology, Beijing, China
[d] School of Architecture, Hang Lung Center for Real Estate, Tsinghua University, Beijing, China

ARTICLE INFO

Keywords:
Emergency Medical Services (EMS) accessibility
Older adults
Ambulance trafficability
Pre-hospital time
Deep learning
Street view images

ABSTRACT

Rapid urbanization and population aging have made equitable Emergency Medical Services (EMS) access for older adults a critical challenge in high-density cities. This study develops a deep learning framework to evaluate EMS accessibility, considering ambulance trafficability derived from street view images (SVIs). A Multi-Scale Vision Transformer (MSViT) model classifies SVIs into impassable, narrow, and passable categories to assess road conditions. Travel speeds are then assigned based on the classified trafficability and road hierarchy data. The framework measures the pre-hospital time through two-stage travel (emergency center-to-patient and patient-to-hospital), while evaluating accessibility through two complementary metrics: the inverse of the shortest total pre-hospital time, and a composite accessibility score with Gaussian time-decay weighting for all facilities within 15-minute service ranges. A case study in Beijing's Old City demonstrated that considering ambulance trafficability reduces the estimated 15-minute coverage from 94.18 % to 83.14 %, revealing significant overestimation when road conditions are neglected. Spatially, peripheral areas achieved better nearest-facility response times, whereas central regions dominated in comprehensive service coverage. Additionally, EMS accessibility patterns strongly correlated with older adults' distribution, showing limited income-based disparities. This study shifts the focus from supply-demand balancing to road system management in EMS accessibility, which can be integrated with existing methods to support more sustainable and targeted infrastructure optimization in aging cities.

1. Introduction

With the global trend of population aging, ensuring the accessibility of emergency medical services (EMS) for older adults has become increasingly critical (Hashtarkhani et al., 2020; Hjalmarsson et al., 2020). According to the World Health Organization (2024), the population aged 60 years and over is projected to reach 2.1 billion by 2050, with the proportion increasing from 12 % in 2015 to 22 % by 2050. Due to the decline in physical functions and weakened immune systems, older adults are more susceptible to various acute and chronic diseases, which makes them highly dependent on medical facilities (Dinh et al., 2016; Lowthian et al., 2011). Among these, EMS holds particular importance, as timely access to emergency care can significantly reduce mortality from acute conditions such as strokes, heart attacks, and fractures, thereby improving the quality of life for older adults (Mackenzie, 2018; Wilson et al., 2015). Consequently, the equitable and efficient accessibility of EMS for this vulnerable population has emerged as a critical issue for sustainable urban renewal and healthcare system improvement (Keskinoglu et al., 2010; Zhu et al., 2021).

Despite the growing demand for EMS among older adults, existing methods for assessing EMS accessibility often fall short in capturing the complexities of real-world urban environments regarding ambulance trafficability. Traditional methods for assessing EMS accessibility, such as gravity models, Floating Catchment Area (FCA) methods, and their variants, primarily focus on the balance between supply and demand (Liu et al., 2025; Piovani et al., 2018; Stacherl & Sauzet, 2023), often using fixed thresholds like 15-minute or 8-minute response times to evaluate service coverage and equity (Coles et al., 2017; Cui et al., 2021; Liu et al., 2022; Shen et al., 2021). While these approaches provide valuable insights, they tend to overlook road conditions, particularly the

* Corresponding author at: Room 410, Beijing University of Technology, No.100 Pingleyuan, Chaoyang District, Beijing, 100124, China.
E-mail address: enjiazhang@bjut.edu.cn (E. Zhang).

https://doi.org/10.1016/j.scs.2025.106804
Received 10 March 2025; Received in revised form 6 September 2025; Accepted 7 September 2025
Available online 8 September 2025

real-world trafficability of ambulances on urban road networks. Recent advancements in big data and positioning technologies, like Web Mapping APIs and GPS-tracked data, have enabled the incorporation of dynamic real-time travel time into EMS evaluations (Park & Goldberg, 2021; Su et al., 2022; Wang et al., 2022). However, in actual EMS scenarios, ambulances often have priority access to roads, and their travel speeds are less affected by dynamic congestion than private vehicles, particularly when emergency green corridors with traffic control measures are implemented. Nevertheless, lower-class roads in high-density urban areas are frequently obstructed by parked vehicles and other persistent obstacles, which can hinder ambulance passage far more than dynamic congestion. Additionally, non-vehicular solutions—such as stretcher-carrying through narrow pathways—are often neglected in current studies. Therefore, incorporating ambulance accessibility considerations—particularly for older adults' emergency care needs—holds significant implications for sustainable urban renewal and precision governance in high-density areas (Zhang et al., 2024b).

SVIs provide a detailed, ground-level perspective of road conditions (Chen et al., 2023; Rzotkiewicz et al., 2018; Ye et al., 2025; Zhang et al., 2023), offering unique insights into the factors that influence EMS accessibility, particularly in high-density urban environments where road conditions can be highly variable and complicated. Unlike traditional accessibility analysis methods, which often rely on generalized assumptions about road conditions, SVIs provide visual information on the state of urban infrastructure, including details such as road surfaces, obstacles (e.g., parked cars, construction work, and road maintenance), street furniture, and temporary construction (Isola et al., 2019; Marasinghe et al., 2024), all of which can significantly impact ambulance travel times. Additionally, SVIs record a wide range of road characteristics, such as road damage, street width, lane availability, and the presence of non-motorized traffic, providing a more holistic view of accessibility challenges (Hacıefendioğlu & Başağa, 2022; Toney et al., 2024). By applying advanced deep learning techniques to SVIs, we can not only detect and classify these road features but also assess their potential impact on ambulance trafficability, thereby enabling a more precise and context-specific evaluation of EMS accessibility.

Therefore, this study bridges a key gap in EMS research—the lack of built environment consideration for ambulance trafficability—by integrating deep learning-based analysis of street-level images, accounting for factors critical to ambulance mobility, such as road width and traffic constraints. Using the high-density Old City of Beijing as a case study, we established a Multi-Scale Vision Transformer (MSViT)-based framework to identify areas where emergency services are inadequately provided. Given the higher likelihood of EMS demand in areas with concentrated elderly populations, we focused specifically on geriatric emergency services, providing actionable insights for urban planners and EMS providers to optimize service delivery. This framework is expected to help improve EMS efficiency by revealing how urban roads impact emergency outcomes and guide sustainable city planning for safer, more resilient healthcare access.

The remainder of this study is structured as follows: Section 2 reviews state-of-the-art studies on EMS accessibility measurements and the potential use of SVIs in improving accuracy. Section 3 details the study area, data sources, analytical framework, and detailed methods. Section 4 presents empirical results on spatial equity and efficiency of EMS delivery for older adults. Finally, we discuss the study's contributions, integration potential with existing methods, policy implications, and limitations, followed by a conclusion summarizing key findings.

2. Literature review

2.1. Evaluation methods for EMS accessibility

Over the years, a variety of approaches have been proposed to assess EMS accessibility, focusing on the spatial distribution of both EMS resources and demand (Hashtarkhani et al., 2020; Ventura et al., 2022). Gravity models or potential models, which highlight the connection between the supply of medical services and the demand from patients, have been extensively applied in measuring hospital accessibility (Piovani et al., 2018; Stacherl & Sauzet, 2023). Based on gravity models, the Floating Catchment Area method, along with its extended versions, such as the Two-Step Floating Catchment Area (2SFCA) (Jin et al., 2022; Luo & Wang, 2003), improved 2SFCA with distance decay function (Liu et al., 2023), dynamic considerations (Javanmard et al., 2024), involving competition among demand or supply nodes (Delamater, 2013), multiple travel means (Mao & Nekorchuk, 2013), and considering the distance preference of patients (Shen et al., 2021), have been widely used and improved to assess EMS allocation. These approaches measure the overlap between the supply of medical facilities (e.g., hospitals, EMS stations) with the spatial distribution of potential demand (e.g., population density) to identify areas with insufficient emergency services, evaluate the spatial equity of healthcare resources (Deng et al., 2021; Liu et al., 2025; Seong et al., 2024; Wang et al., 2021), and allocate resources to emergencies and stations (Hannoun & Menéndez, 2022).

Recent studies have increasingly incorporated road trafficability—defined as the capacity of vehicles, especially ambulances, to traverse urban road networks efficiently—into their analyses of emergency response systems. Comparising to early studies considering the road hierarchies—such as arterial roads, collector streets, and local roads—as factors that influence the trafficability and speed of private vehicles and ambulances (Cho & Yoon, 2015; Lee et al., 2018), recent studies focus more on the traffic congestion, road conditions, and other obstacles like parked cars or road closures can significantly impact ambulance travel times. For example, graph neural network (GNN)-based approaches for rapid seismic reliability assessment of highway bridge systems (Liu & Meidani, 2024) and for travel distance estimation and route recommendation under probabilistic hazards (Liu & Meidani, 2025), which offer a novel method for large-scale network analysis of transportation system reliability in the face of large-scale disasters.

Most studies incorporate real-time traffic data to improve the accuracy of EMS travel time models. Web Mapping APIs on digital navigation maps or real ambulance-traced GPS data have been utilized to evaluate travel times, accounting for real-time traffic congestion, road hierarchy, and other dynamic factors (Olivier et al., 2022; Su et al., 2022; Xu et al., 2022). These studies measured the EMS delay (Zhang et al., 2024b) and coverage (Hu et al., 2020), compared the differences with the use of lights and sirens (Fleischman et al., 2013), estimated travel time in the process of emergency (Su et al., 2022; Xu et al., 2022) during daylight, rush-hour intervals and midnight, and evaluated temporal variations in healthcare accessibility and their impact on horizontal and vertical equity (Yang et al., 2024). By combining these metrics, researchers approximate the actual time cost of vehicle travel across diverse urban settings.

In these studies, considerations of EMS accessibility, compared to primary care, place greater emphasis on the shorter response time required for emergencies. This leads to the establishment of a threshold or buffer zone, such as a 15-minute first aid circle (Cui et al., 2021) and an 8-minute golden time circle (Coles et al., 2017; Shen et al., 2021), to evaluate the extent of facility coverage and the balance between supply and demand (Pedigo & Odoi, 2010; Shin & Lee, 2018). However, most studies still focus on the trafficability of private vehicles, which have different priorities and constraints with ambulances. For example, ambulances often have priority access on roads, which can mitigate the effects of congestion. Moreover, high-density urban areas frequently have obstacles on lower-class roads—such as parked cars, narrow lanes, and construction zones—that can impede ambulance travel far more than congestion during non-peak hours (Zhang et al., 2024b). These factors are particularly important for EMS systems that serve vulnerable populations, such as older adults, who are more likely to live in dense, urban areas where road conditions and accessibility may vary greatly.

2.2. Road condition assessment using SVIs and deep learning methods

Road conditions, including surface quality and roadway width, constitute critical determinants of emergency access efficiency (El-Maissi et al., 2023) are often ignored in EMS accessibility measurement. SVIs offer a highly detailed, ground-level perspective of road conditions, providing valuable insights for the assessment of road quality and identification of potential defects that may hinder vehicle passage, including ambulances. These images are particularly effective for evaluating elements such as road surfaces, obstacles, traffic signs, street furniture, and the general condition of urban infrastructure (Chen et al., 2023; Zhang et al., 2023). Various advanced techniques, such as semantic segmentation, object detection, and image classification, are commonly employed to detect and categorize these issues (Zhang et al., 2024a). Specifically, deep learning models like Faster R-CNN (Hacıefendioğlu & Başağa, 2022), SSD (Toney et al., 2024), and the YOLO series (Jiang et al., 2022) have been widely applied to detect road damage, identify on-road object, measure the walkability (Li et al., 2022), and identify and delineate key street elements, including cycleways (Wei et al., 2025), trees, traffic signs, and other potential obstructions, facilitating the creation of comprehensive inventories that help better understand factors that might impede or delay vehicle movement (Lumnitz et al., 2021). Numerous studies in transportation field highlight how certain street features (e.g., the presence, condition, and quality of bicycle lanes, sidewalks, and road surfaces) can either enhance or hinder pedestrian safety, providing critical data to inform urban infrastructure improvements (Isola et al., 2019; Johnson & Gabler, 2015; Kwon & Cho, 2020).

A more recent study utilized SVIs with an improved Vision Transformer (ViT) model to assess ambulance trafficability, specifically in terms of the ability of ambulances to navigate urban streets in emergencies (Pan et al., 2024). By evaluating road trafficability considering factors such as street width, the placement of objects (e.g., obstructive parking along the axis and trash bins scattered in narrow alleys), and temporary roadworks or construction, the study demonstrated how these elements can significantly impact an ambulance's passability. Building upon Pan et al.'s methodological advancements, this study developed a novel approach for calculating pre-hospital time and measuring EMS accessibility for older adults, informing sustainable urban renewal, particularly for equitable emergency coverage and resilient health infrastructure development in high-density built urban areas.

3. Methods

3.1. Study area and data sources

The study focuses on the historic urban core of Beijing, the area within the Second Ring Road, as shown in Fig. 1. This region, as Beijing's old city, features a complex high-density urban fabric shaped by centuries of development and serves as a residence for a significant proportion of the elderly population. The intricate street network, historical infrastructure, and dense population make this area an ideal case study for analyzing the complex EMS accessibility with a focus on ambulance trafficability.

Our study primarily relied on SVIs sourced from Baidu Maps (one of China's largest digital navigation maps, https://map.baidu.com) to assess ambulance trafficability using machine learning methods. Specifically, the goal is to analyze and classify the ability of ambulances to navigate streets based on SVIs. Unlike previous studies collecting SVIs every 50 m (Zhang et al., 2023), we sampled SVIs at 25 m intervals along roads within the analysis area and captured the forward-facing and backward-facing view images along the road at each sampling point in July 2024 to achieve higher accuracy (see Note 1 in the Supplementary Material (SM) for a comparison of different sampling distances). Therefore, the spatial resolution of road trafficability analysis in this

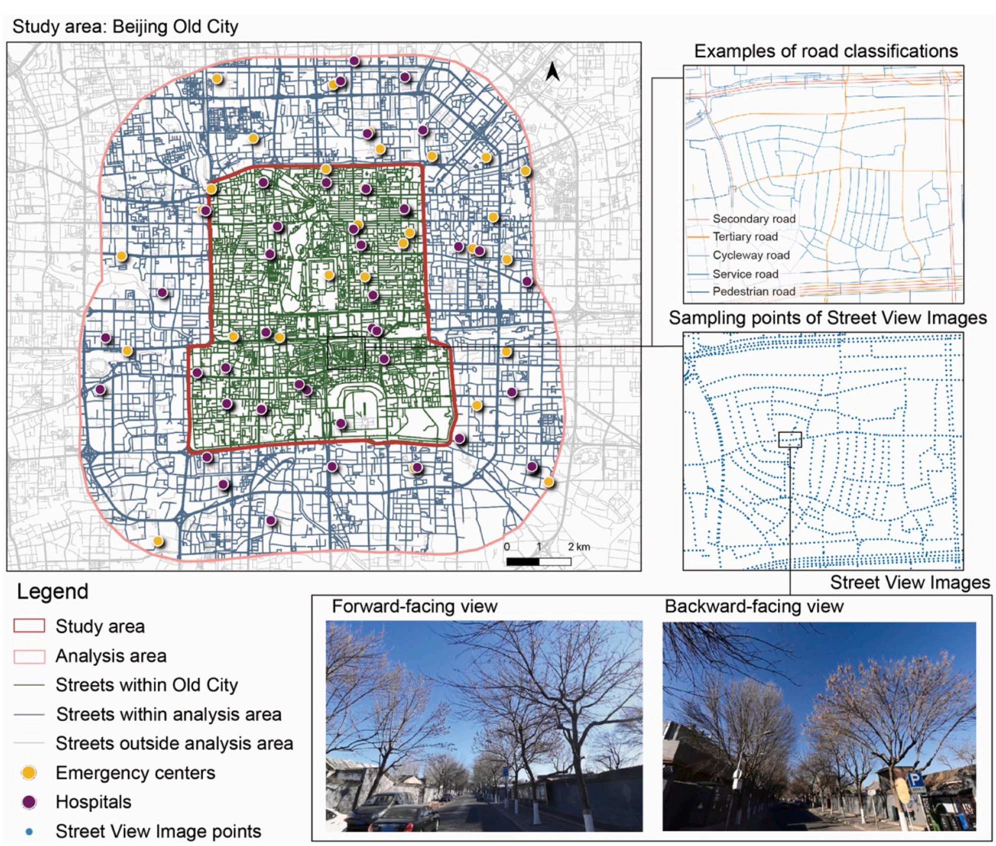

Fig. 1. Study area and examples of road classifications and street view images.

study is 12.5 m.

In addition to SVIs, this study integrated several complementary datasets. Road network data accessed in 2023 from OpenStreetMap (OSM) (https://www.openstreetmap.org/) provided detailed information on street connectivity and hierarchy, forming the spatial framework for evaluating ambulance routes. Locations of emergency center stations and hospitals were obtained in 2023 from Gaode Maps (https://www.amap.com/), ensuring an accurate representation of medical facilities within and around the study area. Elderly population (age≥60, 2020) data was sourced from WorldPop (https://www.worldpop.org/)'s high-resolution (100 m × 100 m) demographic datasets. Additionally, income data at the neighborhood scale (2020) was obtained from Baidu Huiyan (https://huiyan.baidu.com/), with elderly individuals categorized into three quantile-based groups: low (bottom 25 %), middle (25 %–75 %), and high income (top 25 %). This multidimensional data integration supported comprehensive evaluations of both efficiency and equity in EMS accessibility.

To ensure accurate identification of the nearest emergency stations and hospitals for areas along the edges of the Second Ring Road, we extended the data collection beyond the boundaries of the study area. The extension process involved calculating the nearest emergency stations and hospitals for the outermost grid surrounding the Second Ring Road. For the selected emergency stations, we determined the longest route extending outside the Second Ring Road and used the distance of this route as a radius to create a buffer zone that extended outward. This buffer zone ensured comprehensive data coverage for SVIs, road networks, and emergency facilities within the analysis area (Fig. 1). This approach allowed us to capture not only the core urban area's complexity but also the potential accessibility challenges in peripheral zones, enhancing the robustness of our analysis.

3.2. Research framework

This study proposed a six-step framework to assess the accessibility of EMS for older adults, considering ambulance trafficability, as illustrated in Fig. 2. The first step involved acquiring SVIs. A total of 292,008 SVIs were collected from 146,004 sampling points within the analysis area. Of these, 3600 representative road images were selected for training a deep learning model, while the remaining images were designated as prediction data.

In the second step, the selected dataset was labeled through a two-stage process: pre-labeling and formal labeling. During pre-labeling, 3600 images were roughly classified into three categories to ensure balanced data. For formal labeling, five experienced ambulance drivers (averaging 12.7 years of EMS experience) were recruited to label the images based on the dimensions of a Mercedes-Benz Vito 119 ambulance (5223 mm × 1901 mm × 2301 mm). The images were categorized into three distinct classes according to the level of road accessibility for ambulances (Table 1). The first category (Class 0, impassable) included roads deemed entirely impassable due to severe obstructions, such as permanent barriers, streets fully occupied by parked vehicles, or extremely narrow alleys that do not meet the width requirements for ambulance passage. The second category (Class 1, narrow) represented roads that were technically passable but posed significant challenges, including those narrowed by temporary obstacles such as parked cars, delivery vehicles, or construction materials. These roads required ambulances to maneuver carefully, potentially slowing their progress and increasing response times. The third category (Class 2, passable) encompassed fully passable roads without any obstructions, offering ideal conditions for ambulance travel with sufficient width and clearance, ensuring smooth navigation at optimal speeds. To mitigate potential labeling bias arising from individual subjectivity, this study exclusively utilized images with consistent annotations across all participating driver volunteers. Specifically, any images exhibiting inter-rater labeling discrepancies were systematically discarded during dataset construction. The final curated dataset comprised 3199 unanimously labeled samples for model training.

In the third step, the labeled dataset was divided into a training set (70 %) and a test set (30 %) for model development and validation. The fourth step focused on training an improved MSViT model for classification tasks based on Pan et al. (2024)' lightweight Vision Transformer model. This model was trained on the labeled dataset and then used to predict the trafficability classification for the remaining SVIs. The model output provided a classification for each image into one of the three categories, enabling a comprehensive assessment of ambulance trafficability at all sampling points.

In the fifth step, the trafficability results were integrated with road network data to calculate pre-hospital time and evaluate EMS accessibility at a 100 m × 100 m grid resolution. Road networks were split into 25-meter street segments based on SVI sampling points, with each

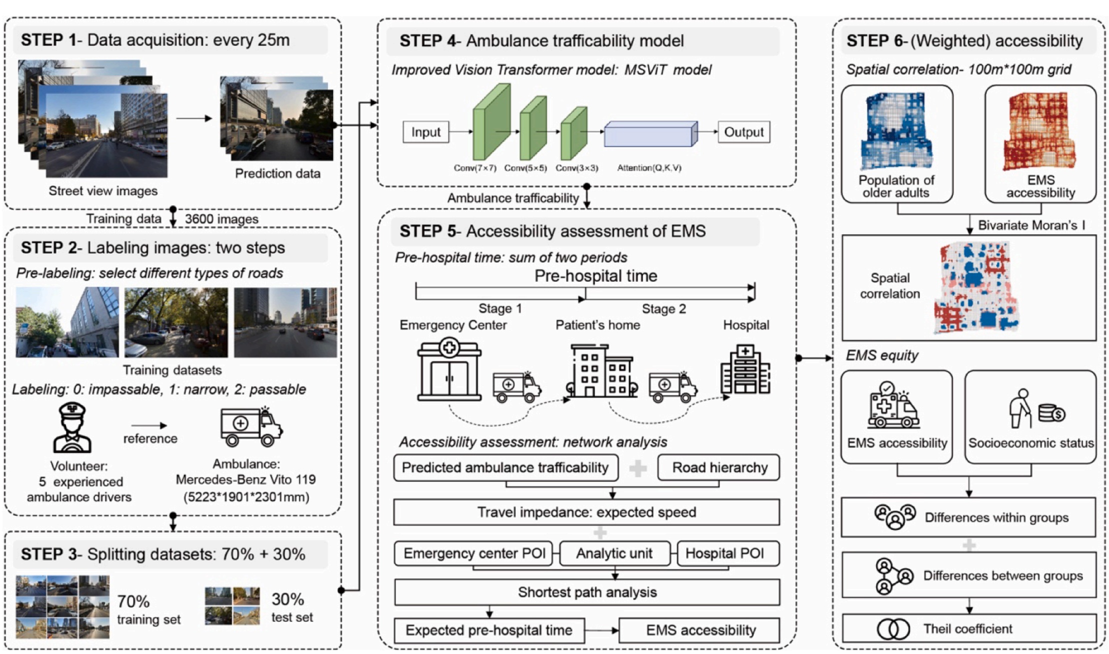

Fig. 2. Research framework.

Table 1
Examples of labelled different road trafficability for ambulances.

Category	Examples	Descriptions
Impassable (1,315)	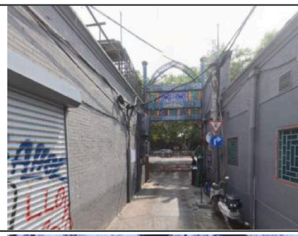 	With severe obstructions, occupied by parked vehicles, or not meeting the width requirements for ambulance passage.
Narrow (882)	 	Technically passable but narrowed by temporary obstacles such as parked cars, delivery vehicles, or construction materials.
Passable (1,002)	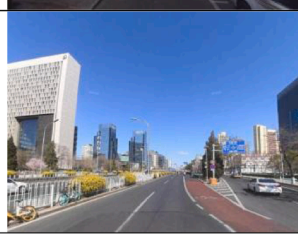 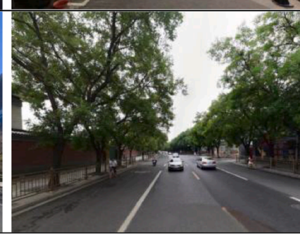	Without any obstructions, offering ideal conditions for ambulance travel with sufficient width and clearance.

segment adopting the poorer accessibility result (i.e., the smaller value) from the two SVI measurements at each sampling point. Pre-hospital time was calculated through two stages: the travel time from the emergency center to the patient's location, and from the patient's location to the hospital. Using the predicted trafficability classifications and road hierarchy, this study estimated travel impedance—the expected speeds—for road segments according to the *Technical Standard of Highway Engineering* (Ministry of Transport of People's Republic of China, 2014) and the *Evaluation Methods for Road Traffic Congestion Levels* (National Technical Committee 576 on Traffic Management of Standardization Administration of China, 2020). For areas impassable to ambulances, emergency personnel typically resort to transporting patients using stretchers or ambulance beds, which corresponds to walking speeds. For narrow streets, we weighted the travel speed based on the coefficient of moderate congestion (see **Table S1** in SM for the designed and adjusted speed for different road hierarchies). These parameters were incorporated into ArcGIS's network analysis module to calculate the shortest pre-hospital time, weighted by expected speeds, between emergency centers, grid centroids, and hospitals. Then, we proposed two complementary indicators to evaluate the EMS accessibility. Additionally, we conducted comparative analyses between our trafficability-informed results and conventional models that assume designed speeds without accounting for ambulance-specific road constraints.

The final step involved spatial and economic analyses to evaluate the equity of EMS accessibility for older adults. A bivariate Moran's I analysis was conducted to examine the spatial correlation between EMS accessibility and elderly population distribution using WorldPop data. Additionally, the study analyzed the EMS accessibility of elderly populations with different economic characteristics to assess equity. This was achieved using the Theil index, which decomposes inequalities into within-group and between-group disparities, as well as an overall Theil index. This approach provided a quantitative measure of inequities in EMS accessibility, capturing both intra-group variations among elderly populations with similar economic characteristics and inter-group differences across populations with differing attributes.

3.3. Methods

(1) Optimized MSViT model

This paper referenced the Vision Transformer model proposed by Pan et al. (2024), which featured four attention heads and one sequential encoder. To further improve the model's convergence speed and reduce training time, a multi-scale convolutional stacked layer (Yan et al., 2024) was introduced to optimize the model. The input layer of the optimized MSViT consisted of three convolutional layers with different scales: the first layer had a kernel size of 7×7 with a stride of 1×1, the second layer had a kernel size of 5×5 with a stride of 2×2, and the third layer had a kernel size of 3×3 with a stride of 2×2. Each convolutional layer was followed by a batch normalization layer and a Gaussian Error Linear Unit (GELU) activation function layer. In contrast, the original ViT's input layer contained only a single convolutional layer with a kernel size of 4×4 and a stride of 4×4.

To compare the performance and convergence speed between MSViT and the original ViT, both models were trained under identical conditions. The dataset consisted of a training set containing 920 impassable, 617 narrow, and 701 passable road images, along with a test set comprising 395 impassable, 265 narrow, and 301 passable road images. An early stopping mechanism was implemented, which halted training if the model's loss function did not decrease for five consecutive epochs. Additionally, to evaluate the impact of the early stopping mechanism on model performance, the original ViT without this mechanism was also included in the experiments. Two metrics were used to assess the performance of each model: accuracy, which evaluated the model's average performance across all categories, and the F1 score, which represented the harmonic mean of precision and recall for each category. Meanwhile, two other metrics were employed to evaluate the models' convergence speed: the number of convergence epochs and the training time.

The model training results are shown in Table 2. The original ViT, trained without early stopping, completed 100 epochs in 37 min and achieved an accuracy of 0.757. With early stopping enabled, it converged after 82 epochs in 32 min, reaching an accuracy of 0.753. In contrast, MSViT with early stopping converged after only 42 epochs in 18 min, achieving an accuracy of 0.766. This demonstrates that the specialized design of MSViT significantly improved convergence speed and reduced training time through structural optimization while maintaining model performance. In terms of recognition performance across different categories, as evaluated by the F1 score, MSViT achieved 0.821 for impassable, 0.553 for narrow, and 0.846 for passable. The lower performance in recognizing narrow roads stems from their hybrid characteristics—they share some features with both impassable and passable categories, making them prone to misclassification. The confusion matrix of MSViT (Fig. 3) reveals this trend, with the diagonal elements being recall rates. As shown in Fig. 3, the narrow category was frequently misclassified as impassable or passable, leading to its lower recognition performance. In some cases, the model correctly identified the road as narrow but failed to determine whether it was suitable for ambulance passage, leading to confusion between narrow and impassable. In other cases, the model recognized that the road met the conditions for ambulance passage but inaccurately assessed its width, resulting in confusion between narrow and passable.

The trained MSViT model was then applied to the full dataset for prediction. The final classification results indicated that 68,339 images (23.4 %) were classified as impassable, 68,925 images (23.6 %) as narrow, and 154,744 images (53.0 %) as passable. These results provided an overview of ambulance trafficability across the analysis area, highlighting the distribution of road conditions that can impact EMS accessibility.

(2) Integrated pre-hospital emergency accessibility measurement

According to the definition of spatial accessibility, the closer two nodes are in space, the shorter the travel time, resulting in a higher spatial accessibility value. Therefore, considering the actual travel conditions for emergency vehicles to determine the travel impedance, this study employed the shortest path analysis to calculate the travel times from each emergency station to analytic grids and from analytic grids to hospitals. We used two complementary indicators to measure accessibility: (1) a shortest-path analysis considering only the fastest routes, and (2) a composite accessibility index incorporating Gaussian decay effects across multiple facilities within 15-minute service coverage areas:

$$A_j = \frac{1}{\min\left(T_{ij} + T_{jk}\right)} \quad (1)$$

$$GA_j = \sum_{i \in I} e^{-\frac{1}{2}\left(\frac{T_{ij}}{T}\right)^2} + \sum_{k \in K} e^{-\frac{1}{2}\left(\frac{T_{jk}}{T}\right)^2} \quad (2)$$

where, A_j and GA_j represent the fastest and Gaussian-integrated pre-hospital EMS accessibility for grid j, with higher values indicating better accessibility. T_{ij} is the travel time from emergency station i to grid j, T_{jk} is the travel time from grid j to hospital k, T is set as 8 min, which indicates the golden time for time-sensitive emergencies, I and K are the sets of emergency stations and hospitals within 15-minute transfer ranges.

(3) Bivariate Moran's I for the correlation between older adult population and accessibility

To optimize the allocation of emergency medical resources, this study utilized the bivariate Moran's I to assess the spatial relationship between the distribution of the older adult population and EMS accessibility. The bivariate Moran's I can be divided into global and local indices, with the specific formulas as follows:

$$I = \frac{N\sum_i\sum_j w_{ij}\left(E_i - \overline{E}\right)\left(A_j - \overline{A}\right)}{\sqrt{\sum_i\left(E_i - \overline{E}\right)^2 \times \sum_j\left(A_j - \overline{A}\right)^2}} \quad (3)$$

$$I_i = \frac{\left(E_i - \overline{E}\right)\sum_j w_{ij}\left(A_j - \overline{A}\right)}{\sqrt{\frac{\sum_i\left(E_i - \overline{E}\right)^2}{N}} \times \sqrt{\frac{\sum_j\left(A_j - \overline{A}\right)^2}{N}}} \quad (4)$$

where, I indicates the global bivariate Moran's I, I_i represents the local bivariate Moran's I for the i th spatial unit, E_i is older adult population at grid i, A_j is the EMS accessibility at grid j, $\overline{E}$ and $\overline{A}$ are the mean values of the older adults population and EMS accessibility, respectively, w_{ij} is the spatial weight matrix, representing the spatial relationship between spatial units i and j, N is the number of grids within the study area.

The global bivariate Moran's I measures the overall spatial correlation between two attributes, with values ranging from −1 to 1. Higher absolute values indicate a stronger spatial correlation. To determine the statistical significance of the global bivariate Moran's I, this study employs a 5 % significance level. The local bivariate Moran's I complements the global measure by identifying spatial patterns and variations at the local level. The resulting local patterns are typically categorized into four types of spatial clustering: high-high, low-low, high-low, and low-high. These detailed local insights are crucial for understanding spatial heterogeneity and guiding targeted interventions or policy decisions.

(4) Theil Coefficient

This study employed the quantile method to classify the grids within the Second Ring Road into three income-based groups for elderly populations: low income (bottom 25 %), middle income (25 %−75 %), and high income (top 25 %). On this basis, the Theil coefficient was used to evaluate the equity of pre-hospital care accessibility among elderly individuals at different income levels, which provides a comprehensive measure of overall inequality and decomposes inequality into within-group and between-group components. The Theil coefficient ranges from 0 to 1, where a value of 0 indicates perfect equity (resources are evenly distributed), and higher values signify greater inequity in resource allocation. The Theil coefficient, within-group inequality, and between-group inequality are calculated as:

$$T = \frac{1}{N}\sum_{i=1}^{N}\frac{A_i}{\overline{A}}\ln\left(\frac{A_i}{\overline{A}}\right) \quad (5)$$

$$T_w = \sum_{k=1}^{K}\frac{n_k}{N}T_k \quad (6)$$

$$T_b = \sum_{k=1}^{K}\frac{n_k}{N}\frac{\overline{A}_k}{\overline{A}}\ln\left(\frac{\overline{A}_k}{\overline{A}}\right) \quad (7)$$

Table 2
Model training and deployment.

Models	Accuracy	F1 score			Convergence epochs	Training Time (min)
		Impassable	Narrow	Passable		
Original ViT	0.757	0.814	0.551	0.827	100	37
Original ViT-Early Stop	0.753	0.787	0.609	0.837	82	32
MSViT-Early Stop	0.766	0.821	0.553	0.846	42	18

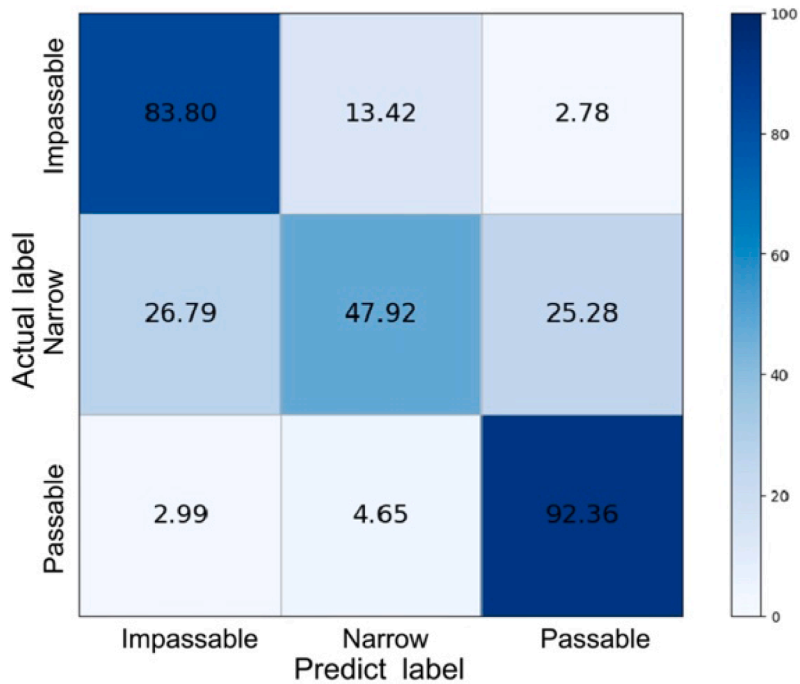

Fig. 3. Confusion matrix of predicted versus actual classifications (%).

where, T is the Theil coefficient, representing overall inequality, T_w is the within-group inequality, T_b is the between-group inequality. N indicates the total number of grids, A_i is the value of EMS accessibility for grid i, $\overline{A}$ is the mean value of EMS accessibility across all grids, k is a specific group, n_k is the number of grids in group k, T_k is the Theil coefficient for group k, calculated using the formula (4), $\overline{A}_k$ is the mean value of EMS accessibility for group k.

4. Results

4.1. Deep learning-based ambulance trafficability

The distribution of ambulance trafficability at the street-segment

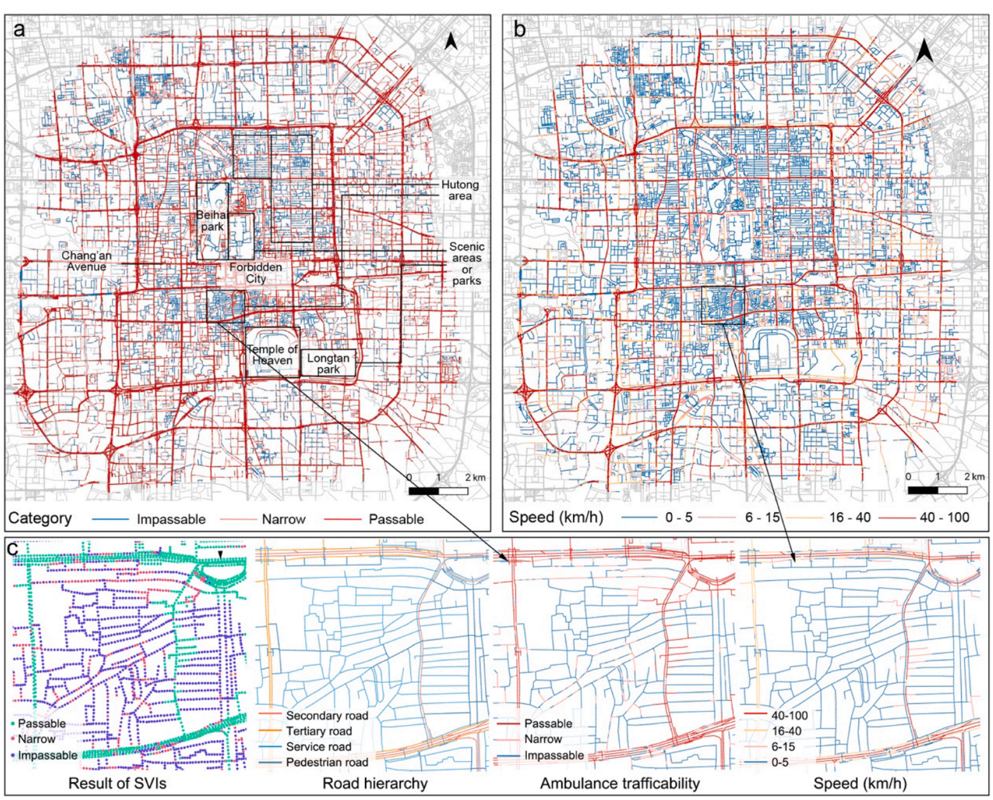

Fig. 4. Ambulance trafficability (a) and traffic speeds (b) based on MSViT model results, with zoomed-in insets showing representative examples (c).

scale is illustrated in Fig. 4-a. The results indicate that ambulance trafficability within the Second Ring Road is relatively poorer compared to areas outside the ring, particularly in *Hutong* areas and within scenic zones, where many regions are impassable to ambulances. In contrast, ring roads exhibit better trafficability. This suggests that, despite the Old City having a higher road density, ambulance trafficability is even worse. The finding further underscores the importance of studying ambulance accessibility within high-density areas, which could be overlooked when only calculating the road network accessibility. Based on ambulance trafficability and road hierarchy, the travel speed of each street segment was calculated. The final distribution of road travel speeds is shown in Fig. 4-b. Major arterial roads and ring roads have relatively higher travel speeds, while speeds within *Hutong* districts are significantly lower (Fig. 4-c).

4.2. Pre-hospital EMS time based on ambulance trafficability

To compare the differences between considering ambulance trafficability and traditional studies, we calculated the pre-hospital time without accounting for ambulance trafficability (Table 3). The result reveals that patient-to-hospital transport times were shorter than emergency center-to-patient response times. For the total pre-hospital duration, 85.06 % of grids were completed within 10 min, while 94.19 % met the 15-minute benchmark.

Based on the MSViT model, the analysis of the time distribution for the first stage, second stage, and total pre-hospital times reveals significant disparities in accessibility, as listed in Table 4. While the second stage, which covers the journey to the hospital, shows a high proportion (51.91 %) of grids with travel times of less than 5 min, indicating good access to hospitals, the first stage, covering the time from emergency stations to grid centers, has a larger proportion (54.25 %) of grids with travel times between 5 and 10 min. This suggests that while hospitals are generally accessible, reaching emergency stations from certain areas presents more significant challenges. Furthermore, the total travel times highlight that over 40 % experience total pre-hospital times within 10 min, 83.14 % within 15 min, with some areas still facing delays of over 15 min. Compared to Table 3, a notable difference is that the number and proportion of trips from emergency stations to grid centers within the 0–10 min range were significantly lower, while the proportions for longer time intervals were considerably higher. A similar distribution is also observed for travel times from grid centers to hospitals. This suggests that neglecting ambulance trafficability on road networks could lead to an overestimation of emergency service accessibility, potentially leading to misguided policy decisions. By capturing potential delays due to road conditions and network constraints, our approach provides a more accurate basis for planning and optimizing EMS deployment.

The visualization of shortest pre-hospital travel times for the two stages was shown in Fig. 5. For the first stage, which measures the shortest travel time from the nearest emergency station to the grid center, it was found that the northeastern and southwestern corners of the Old City typically have travel times of less than 4 min. In contrast, travel times in the southeastern corner and western areas generally range from 4 to 7 min. However, within scenic areas such as the Forbidden City and the Temple of Heaven, travel times exceed 10 min. For the second stage, which represents the travel time from the grid center to the nearest hospital, most grids exhibit travel times of less than 4 min. Exceptions are found in areas north of *Chang'an* Avenue, where travel times range from 4 to 7 min, while scenic zones remain the least accessible, with significantly longer times.

Table 3
Count of grids within different pre-hospital time thresholds without considering trafficability.

Time	Stage 1	Percentage	Stage 2	Percentage	Total	Percentage
[0–5] min	7872	81.36 %	8325	86.05 %	1476	15.26 %
(5–10] min	1489	15.39 %	1056	10.91 %	6753	69.80 %
(10–15] min	166	1.72 %	170	1.76 %	883	9.13 %
(15–20] min	57	0.59 %	57	0.59 %	266	2.75 %
(20–25] min	51	0.53 %	33	0.34 %	108	1.12 %
>25 min	40	0.41 %	34	0.35 %	189	1.95 %

Table 4
Count of grids within different pre-hospital time thresholds.

Time	Stage 1	Percentage	Stage 2	Percentage	Total	Percentage
[0–5] min	3559	36.79 %	5022	51.91 %	312	3.22 %
(5–10] min	5249	54.25 %	4117	42.55 %	3917	40.49 %
(10–15] min	633	6.54 %	385	3.98 %	3815	39.43 %
(15–20] min	132	1.36 %	74	0.76 %	981	10.14 %
(20–25] min	60	0.62 %	48	0.50 %	330	3.41 %
>25 min	42	0.43 %	29	0.30 %	320	3.31 %

4.3. Relationship between the older adult population and EMS accessibility

This study compared the distribution of elderly populations with EMS accessibility to analyze the spatial disparities in EMS accessibility for elderly individuals. The distribution of elderly populations (**Fig. S2** in SM) reveals that the density of elderly individuals is generally higher in the northern part of the city, particularly along and north of *Chang'an* Avenue, with areas near the Second Ring Road exhibiting higher elderly density compared to the inner city. The distribution of fastest and Gaussian-integrated EMS accessibility shows a different pattern (Fig. 6-a,b). The fastest accessibility metric demonstrates superior access in northern and southwestern regions, whereas Gaussian-integrated EMS accessibility reveals higher accessibility values in central urban areas. The results demonstrate that while the northern and southwestern regions benefit from faster emergency response times, the central urban area exhibits superior 15-minute accessibility coverage when evaluated through comprehensive Gaussian-integrated analysis.

The global bivariate Moran's I values for fastest and Gaussian-integrated accessibility are 0.350 ($P < 0.001$, Z-score=38.977) and 0.405 ($P < 0.001$, Z-score=45.257), indicating statistically significant positive spatial correlations between elderly population density and EMS accessibility. This suggests that areas with higher elderly populations are generally associated with better accessibility to pre-hospital care services. The local Moran's I analysis further reveals significant spatial clustering patterns (Fig. 6-c,d). In regions with a high elderly population, there is a high-high cluster of good fastest EMS accessibility in the northeastern and southwestern parts of the city and better Gaussian-integrated EMS accessibility in the central areas. Conversely, areas with a lower elderly population, such as the Forbidden City and Temple of Heaven, exhibit low-low clusters, indicating lower EMS accessibility in these areas. Additionally, high-low clusters, where regions with high elderly populations are adjacent to areas with lower EMS accessibility, are primarily found along the Second Ring Road. This suggests a spatial mismatch between the demand for EMS services and their accessibility in these areas. In contrast, low-high clusters, where areas with lower elderly populations are adjacent to regions with better EMS accessibility, are scattered across various locations. Overall, the spatial clustering is predominantly characterized by high-high and low-low clusters, further validating that the supply and demand for EMS are relatively well-matched in the Old City.

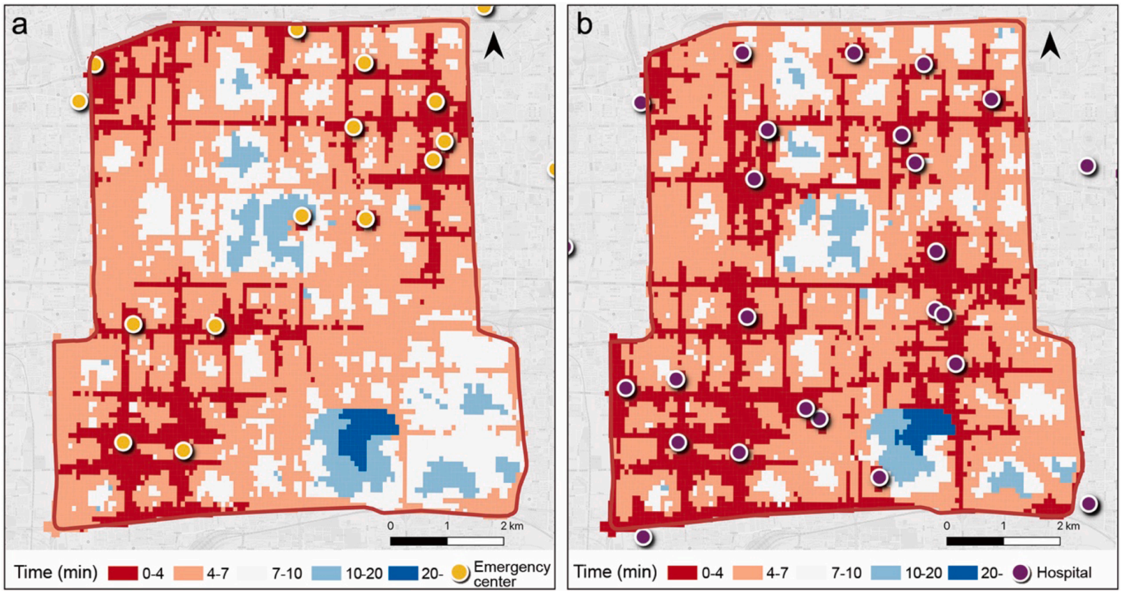

Fig. 5. Time from emergency centers to patients (a) and from patients to hospitals (b).

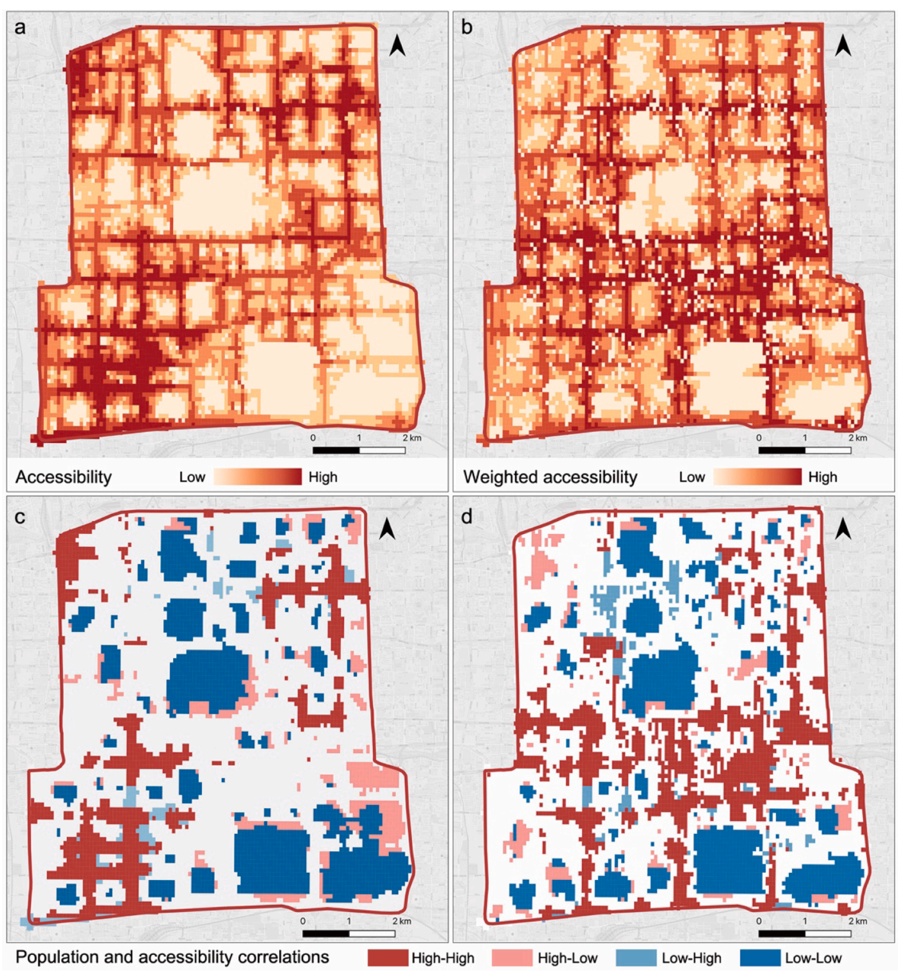

Fig. 6. Spatial distribution of fastest EMS accessibility (a) and Gaussian-integrated accessibility (b), and their spatial correlations with older adults' population (c for fastest accessibility and d for Gaussian-integrated accessibility).

4.4. Equity of EMS accessibility for older adults in different income groups

The analysis of Theil indices reveals distinct patterns of inequality in pre-hospital EMS accessibility for elderly populations across different income groups. As shown in Table 5, while the overall Theil index for fastest accessibility (0.0898) indicates relatively equitable distribution of emergency response capabilities, the substantially higher value for Gaussian-integrated accessibility (0.3027) suggests significant disparities in comprehensive service coverage. Both metrics demonstrate that inequality primarily originates from within-group variations rather than between-group differences, with within-group contributions accounting for 92.88 % and 99.79 % of total inequality for fastest and Gaussian-integrated accessibility, respectively. Notably, middle-income elderly experience the highest inequality in fastest accessibility (Theil=0.0920), while low-income groups face the most pronounced disparities in Gaussian-integrated accessibility (Theil=0.3525), reflecting disparities in road infrastructure quality across neighborhoods. High-income groups show comparatively lower inequality levels across both metrics (0.0578 for fastest and 0.2960 for Gaussian-integrated accessibility). These findings suggest that while current EMS resource allocation does not systematically favor any particular income group, substantial intra-group disparities persist, particularly in terms of comprehensive service coverage for vulnerable populations.

5. Discussions

This study contributes to the field of EMS accessibility assessment by proposing a novel framework that integrates deep learning techniques with SVIs to incorporate the critical factor of ambulance trafficability. Unlike existing studies that often assume uniform road trafficability and constant ambulance speeds (Stacherl & Sauzet, 2023), or rely on private vehicle travel times (Su et al., 2022), our approach explicitly unveiled the impact of road passability on EMS accessibility. By leveraging SVIs and an MSViT model, we provided a granular, ground-level evaluation of ambulance-specific accessibility, directly responding to Zhang et al. (2024b)' finding that the built environment is a key contributor to ambulance delay. This method captured critical factors such as parked cars, road surface conditions, and other potential barriers that directly impact ambulance navigation, which are particularly vital in high-density areas.

This study developed two ambulance-centric accessibility assessment indicators based on total pre-hospital time and Gaussian time-decay weighting, departing from conventional approaches like the 2SFCA method and API-based travel time estimation for two critical reasons. First, older adults rely more on ambulance transport (Keskinoglu et al., 2010), where privileged road access reduces susceptibility to dynamic traffic congestion compared to private vehicles, while making the service more vulnerable to static obstacles, particularly in high-density urban environments. Although API-derived travel times adequately represent private vehicle mobility for primary care cases (Jin et al., 2022; Yang et al., 2024), they fail to capture the unique operational constraints of emergency medical services. Second, unlike mass casualty incidents or patient-initiated facility selection, geriatric EMS demand consists of occasional, sporadic emergencies where the traditional 2SFCA method and its variations—designed for competitive resource allocation (e.g., hospital beds) (Delamater, 2013) and preference-based facility choice (e.g., distance) (Javanmard et al., 2024)—are ill-suited. Since ambulance dispatch and hospital selection are system-controlled rather than patient-driven, and since real-time older adults' EMS demand and spare ambulance numbers are often unavailable, our method to calculate accessibility offers a more operationally realistic approach for geriatric EMS.

Nevertheless, our framework maintains compatibility with existing methods in other emergency services (e.g., police, firefighters, roadside assistance services). It can enhance FCA models through ambulance-specific speed inputs and complement API-based time estimation by providing more accurate estimates in complex, high-density urban environments.

The findings of this study also have important implications for urban planning and EMS policies. By quantitatively demonstrating how road passability critically constrains ambulance mobility in Beijing's high-density urban core, our findings shift the policy focus from traditional supply-demand matching to physical infrastructure optimization. The evidence reveals that targeted improvements in roadway navigability (e.g., clearing static obstructions, optimizing lane configurations) would yield greater EMS efficiency gains than simply adding medical facilities or ambulances in these constrained environments. Additionally, the spatial correlation analysis between elderly population density and EMS accessibility suggests that areas near the Second Ring Road with high demand for EMS services may not always align with the current distribution of emergency facilities. This insight could inform the strategic placement of new emergency stations or the optimization of roads to better match the spatial needs of the elderly population. These insights provide an evidence-based framework for sustainable urban renewal, where emergency accessibility optimization can be integrated with built environment upgrades to create more resilient, age-friendly cities.

Despite these strengths, the study has some limitations. First, the use of static SVIs does not capture real-time changes in road conditions or traffic congestion, which can significantly impact ambulance response times. Future iterations could incorporate real-time ambulance GPS trajectories to monitor actual response patterns, and use active street view acquisition (e.g., quarterly updates) to maintain temporal relevance and identify changes in rapidly evolving urban environments. Second, the spatial resolution of our analysis is limited to 100 m $\times$ 100 m grids, which may not fully account for localized barriers within residential complexes or poorly designed building entrances. Future research could incorporate building-scale data to provide a more detailed understanding of EMS accessibility. Third, the study focuses on a specific urban area (Beijing's Old City), and the applicability of the framework to other high-density cities or regions with different urban structures and traffic conditions needs further validation. Additionally, the current framework cannot discern the legality of parked vehicles—a critical factor affecting ambulance passage in densely built environments where illegally parked cars frequently obstruct emergency routes. Future work could integrate relevant data to provide a more comprehensive evaluation of EMS accessibility and guide more effective urban renewal and fine governance decisions.

6. Conclusion

This study presents a novel framework for assessing the accessibility and equity of EMS for older adults, emphasizing ambulance trafficability through the use of SVIs and deep learning techniques. By employing an improved MSViT model, this study effectively classified SVIs representing road trafficability for ambulances, enabling the assignment of travel speeds to road segments based on observed conditions and hierarchical classifications. This approach addresses a significant gap in existing EMS research, which often overlooks the impact of real-world road conditions on ambulance response times, especially in high-density areas.

Table 5
Theil indices of EMS accessibility for older adults in different income groups.

Results	Fastest accessibility	Gaussian-integrated accessibility
Total_Theil	0.0898	0.3027
Within_group_contribution	92.88 %	99.79 %
Between_group_contribution	6.03 %	0.21 %
High_Incomegroup	0.0578	0.2960
Middle_Incomegroup	0.0920	0.2786
Low_Incomegroup	0.0772	0.3525

Through a case study conducted in Beijing's Old City, the study demonstrated the applicability and effectiveness of this method. The results showed that 83.14 % of analyzed grids met the 15-minute pre-hospital response target when accounting for ambulance trafficability constraints - a significantly lower achievement rate compared to the 94.18 % coverage estimated by conventional models that ignore roadway accessibility factors. This 11.04 percentage point discrepancy demonstrates how traditional approaches potentially overestimate EMS performance by failing to incorporate ground-level mobility barriers. The results revealed distinct spatial patterns in EMS accessibility: peripheral areas showed advantages in nearest-facility response times, while central urban areas demonstrated stronger comprehensive coverage under Gaussian-based accessibility measures. EMS accessibility patterns strongly correlated with older adults' distribution, with small differences between economic groups.

These findings underscore the utility of this framework in providing actionable insights for improving EMS equity and efficiency. By focusing on road-level bottlenecks and the implications for elderly populations, this study provides a basis for urban planners and healthcare policymakers to optimize resource allocation and guide targeted road infrastructure improvements. Importantly, the proposed methodology demonstrates strong complementarity with existing accessibility assessment approaches, which can be adaptively combined with traditional models to inform sustainable urban renewal strategies and create more resilient, safe cities.

CRediT authorship contribution statement

Zhuo Liu: Writing – review & editing, Supervision, Resources, Project administration, Funding acquisition, Conceptualization. **Enjia Zhang:** Writing – original draft, Visualization, Validation, Software, Investigation, Formal analysis, Conceptualization, Data curation. **Shuo Pan:** Writing – review & editing, Software, Formal analysis, Data curation, Methodology. **Sichun Li:** Writing – review & editing, Software, Methodology, Investigation, Formal analysis, Data curation, Conceptualization. **Ying Long:** Writing – review & editing, Conceptualization. **Frank Witlox:** Writing – review & editing, Conceptualization.

Declaration of competing interest

The authors declare that they have no known competing financial interests or personal relationships that could have appeared to influence the work reported in this paper.

Acknowledgments

This work was supported by the National Natural Science Foundation of China [No. 52008006] and the China Scholarship Council [No. 202406540018].

Supplementary materials

Supplementary material associated with this article can be found, in the online version, at doi:10.1016/j.scs.2025.106804.

Data availability

Data will be made available on request.

References

Chen, J., Chen, L., Li, Y., Zhang, W., & Long, Y. (2023). Measuring physical disorder in urban street spaces: A large-scale analysis using street view images and deep learning. *Annals of the American Association of Geographers, 113*(2), 469–487.

Cho, J., & Yoon, Y. (2015). Gis-based analysis on vulnerability of ambulance response coverage to traffic condition: A case study of seoul. Paper presented at the 2015 IEEE 18th International Conference on Intelligent Transportation Systems.

Coles, D., Yu, D., Wilby, R. L., Green, D., & Herring, Z. (2017). Beyond 'flood hotspots': Modelling emergency service accessibility during flooding in York, UK. *Journal of Hydrology, 546*, 419–436.

Cui, E. R., Fernandez, A. R., Zegre-Hemsey, J. K., Grover, J. M., Honvoh, G., Brice, J. H., … Patel, M. D. (2021). Disparities in emergency medical services time intervals for patients with suspected acute coronary syndrome: Findings from the North Carolina prehospital medical information system. *Journal of the American Heart Association, 10* (15), Article e019305. Article.

Delamater, P. L. (2013). Spatial accessibility in suboptimally configured health care systems: A modified two-step floating catchment area (m2sfca) metric. *Health & Place, 24*, 30–43.

Deng, Y., Zhang, Y., & Pan, J. (2021). Optimization for locating emergency medical service facilities: A case study for health planning from China. *Risk Management and Healthcare Policy*, 1791–1802.

Dinh, M. M., Muecke, S., Berendsen Russell, S., Chalkley, D., Bein, K. J., Muscatello, D., … Ivers, R. (2016). Demand for emergency services trends in New South Wales years 2010–2014 (destiny): Age and clinical factors associated with ambulance transportation to emergency departments. *Prehospital Emergency Care, 20*(6), 776–782.

El-Maissi, A. M., Argyroudis, S. A., Kassem, M. M., & Nazri, F. M. (2023). Integrated seismic vulnerability assessment of road network in complex built environment toward more resilient cities. *Sustainable Cities and Society, 89*, Article 104363. Article.

Fleischman, R. J., Lundquist, M., Jui, J., Newgard, C. D., & Warden, C. (2013). Predicting ambulance time of arrival to the emergency department using global positioning system and Google Maps. *Prehospital Emergency Care, 17*(4), 458–465.

Hacıefendioğlu, K., & Başağa, H. B. (2022). Concrete road crack detection using deep learning-based faster r-cnn method. *Iranian Journal of Science and Technology, Transactions of Civil Engineering, 46*(2), 1621–1633.

Hannoun, G. J., & Menéndez, M. (2022). Modular vehicle technology for emergency medical services. *Transportation Research Part C: Emerging Technologies, 140*, Article 103694.

Hashtarkhani, S., Kiani, B., Bergquist, R., Bagheri, N., VafaeiNejad, R., & Tara, M. (2020). An age-integrated approach to improve measurement of potential spatial accessibility to emergency medical services for urban areas. *The International journal of health planning and management, 35*(3), 788–798.

Hjalmarsson, A., Holmberg, M., Asp, M., Östlund, G., Nilsson, K. W., & Kerstis, B. (2020). Characteristic patterns of emergency ambulance assignments for older adults compared with adults requiring emergency care at home in sweden: A total population study. *BMC emergency medicine, 20*(1), 94.

Hu, W., Tan, J., Li, M., Wang, J., & Wang, F. (2020). Impact of traffic on the spatiotemporal variations of spatial accessibility of emergency medical services in inner-city Shanghai. *Environment and Planning B: Urban Analytics and City Science, 47* (5), 841–854.

Isola, P. D., Bogert, J. N., Chapple, K. M., Israr, S., Gillespie, T. L., & Weinberg, J. A. (2019). Google Street View assessment of environmental safety features at the scene of pedestrian automobile injury. *The Journal of Trauma and Acute Care Surgery, 87*(1), 82–86.

Javanmard, R., Lee, J., Kim, K., Park, J., & Diab, E. (2024). Evaluating the impacts of supply-demand dynamics and distance decay effects on public transit project assessment: A study of healthcare accessibility and inequalities. *Journal of Transport Geography, 116*, Article 103833.

Jiang, P., Ergu, D., Liu, F., Cai, Y., & Ma, B. (2022). A review of Yolo algorithm developments. *Procedia Computer Science, 199*, 1066–1073.

Jin, T., Cheng, L., Wang, K., Cao, J., Huang, H., & Witlox, F. (2022). Examining equity in accessibility to multi-tier healthcare services across different income households using estimated travel time. *Transport Policy, 121*, 1–13.

Johnson, N. S., & Gabler, H. C. (2015). Injury outcome in crashes with guardrail end terminals. *Traffic Injury Prevention, 16*(2), S103–S108.

Keskinoglu, P., Sofuoglu, T., Özmen, O., Gündüz, M., & Ozkan, M. (2010). Older people's use of pre-hospital emergency medical services in Izmir, Turkey. *Archives of Gerontology and Geriatrics, 50*(3), 356–360.

Kwon, J.-H., & Cho, G.-H. (2020). An examination of the intersection environment associated with perceived crash risk among school-aged children: Using street-level imagery and computer vision. *Accident Analysis & Prevention, 146*, Article 105716.

Lee, J., Abdel-Aty, M., Cai, Q., & Wang, L. (2018). Effects of emergency medical services times on traffic injury severity: A random effects ordered probit approach. *Traffic Injury Prevention, 19*(6), 577–581.

Li, Y., Yabuki, N., & Fukuda, T. (2022). Measuring visual walkability perception using panoramic street view images, virtual reality, and deep learning. *Sustainable Cities and Society, 86*, Article 104140.

Liu, T., & Meidani, H. (2024). Graph neural network surrogate for seismic reliability analysis of highway bridge systems. *Journal of Infrastructure Systems, 30*(4), Article 05024004.

Liu, T., & Meidani, H. (2025). Graph neural networks for travel distance estimation and route recommendation under probabilistic hazards. *International Journal of Transportation Science and Technology*. https://doi.org/10.1016/j.ijtst.2025.02.006

Liu, Z., Li, S., Cheng, L., Shen, Z., & Witlox, F. (2025). Exploring accessibility to medical facilities for older adults: Potential vs. Revealed accessibility. *Journal of Transport & Health, 40*, Article 101952.

Liu, Z., Li, S., Zhao, X., Wang, Z., & Chen, Y. (2023). Examining accessibility to medical resources for urban older adults with common diseases using multisource data: A case study of Beijing. *Journal of Urban Planning and Development, 149*(4), Article 05023031.

Liu, Z., Zhao, H., Li, S., Chen, Y., & Yao, E. (2022). Understanding evolution process of community-embedded elderly care facilities with big data: A spatiotemporal analytical framework. *Transactions in Urban Data, Science, and Technology, 1*(3–4), 142–163.

Lowthian, J. A., Cameron, P. A., Stoelwinder, J. U., Curtis, A., Currell, A., Cooke, M. W., & McNeil, J. J. (2011). Increasing utilisation of emergency ambulances. *Australian Health Review, 35*(1), 63–69.

Lumnitz, S., Devisscher, T., Mayaud, J. R., Radic, V., Coops, N. C., & Griess, V. C. (2021). Mapping trees along urban street networks with deep learning and street-level imagery. *ISPRS Journal of Photogrammetry and Remote Sensing, 175*, 144–157.

Luo, W., & Wang, F. (2003). Measures of spatial accessibility to health care in a GIS environment: Synthesis and a case study in the Chicago region. *Environment and Planning B: Planning and Design, 30*(6), 865–884.

Mackenzie, R. (2018). *Brief history of pre-hospital emergency medicine, 35* pp. 146–148). BMJ Publishing Group Ltd and the British Association for Accident.

Mao, L., & Nekorchuk, D. (2013). Measuring spatial accessibility to healthcare for populations with multiple transportation modes. *Health & Place, 24*, 115–122.

Marasinghe, R., Yigitcanlar, T., Mayere, S., Washington, T., & Limb, M. (2024). Computer vision applications for urban planning: A systematic review of opportunities and constraints. *Sustainable Cities and Society, 100*, Article 105047.

Ministry of Transport of People's Republic of China. (2014). *Technical Standard of Highway Engineering (JTG B01-2014)*. Beijing, China: People's Traffic Press.

National Technical Committee 576 on Traffic Management of Standardization Administration of China. (2020). *Evaluation Methods for Road Traffic Congestion Levels (GA/T 115-2020)*. Beijing, China: Standards Press of China.

Olivier, A., Adams, M., Mohammadi, S., Smyth, A., Thomson, K., Kepler, T., & Dadlani, M. (2022). Data analytics for improved closest hospital suggestion for EMS operations in New York City. *Sustainable Cities and Society, 86*, Article 104104.

Pan, S., Liu, Z., Yan, H., Chen, N., Zhao, X., Li, S., & Witlox, F. (2024). Automatic identification of bottlenecks for ambulance passage on urban streets: A deep learning-based approach. *Advanced Engineering Informatics, 62*, Article 102931.

Park, J., & Goldberg, D. W. (2021). A review of recent spatial accessibility studies that benefitted from advanced geospatial information: Multimodal transportation and spatiotemporal disaggregation. *ISPRS International Journal of Geo-Information, 10*(8), 532.

Pedigo, A. S., & Odoi, A. (2010). Investigation of disparities in geographic accessibility to emergency stroke and myocardial infarction care in East Tennessee using geographic information systems and network analysis. *Annals of Epidemiology, 20*(12), 924–930.

Piovani, D., Arcaute, E., Uchoa, G., Wilson, A., & Batty, M. (2018). Measuring accessibility using gravity and radiation models. *Royal Society Open Science, 5*(9).

Rzotkiewicz, A., Pearson, A. L., Dougherty, B. V., Shortridge, A., & Wilson, N. (2018). Systematic review of the use of google street view in health research: Major themes, strengths, weaknesses and possibilities for future research. *Health & place, 52*, 240–246.

Seong, K., Jiao, J., Mandalapu, A., & Niyogi, D. (2024). Spatio-temporal patterns of heat index and heat-related emergency medical services (EMS). *Sustainable Cities and Society, 111*, Article 105562.

Shen, Z., Gao, G., & Wang, Z. (2021). Accessibility assessment of prehospital emergency medical services considering supply-demand differences. *Journal of Advanced Transportation, 2021*(1), Article 1925354.

Shin, K., & Lee, T. (2018). Improving the measurement of the Korean emergency medical system's spatial accessibility. *Applied Geography, 100*, 30–38.

Stacherl, B., & Sauzet, O. (2023). Gravity models for potential spatial healthcare access measurement: A systematic methodological review. *International Journal of Health Geographics, 22*(1), 34.

Su, Y., Wang, J., Wang, J., & Wang, G. (2022). Measuring spatial accessibility to hospitals of acute myocardial infarction in multi period scale: A case study in Shijingshan district, Beijing, China. *ISPRS International Journal of Geo-Information, 11*(2), 137.

Toney, G., Sethi, G., Bhargava, C., & Salian, V. (2024). Modified ssd framework for on-road object detection. *Intelligent circuits and systems for sdg 3–good health and well-being* (pp. 331–340). CRC Press.

Ventura, C. A. I., Denton, E. E., David, J. A., Schoenfelder, B. J., Mela, L., Lumia, R. P., … Haldar, B. (2022). Emergency medical services prehospital response to the covid-19 pandemic in the us: A brief literature review. *Open Access Emergency Medicine*, 249–272.

Wang, J., Su, Y., Chen, Z., Tang, L., Wang, G., & Wang, J. (2022). Assessing the spatial accessibility of urban medical facilities in multi-level and multi-period scales based on web mapping API and an improved potential model. *ISPRS International Journal of Geo-Information, 11*(11), 545.

Wang, K., Bai, J., & Dang, X. (2021). Spatial difference and equity analysis for accessibility to three-level medical services based on actual medical behavior in Shaanxi, China. *International Journal of Environmental Research and Public Health, 18*(1), 112.

Wei, X., Li, J., Zhang, X., Gu, H., Van de Weghe, N., & Huang, H. (2025). An innovative framework combining a CNN-Transformer multiscale fusion network and spatial analysis for cycleway extraction using street view images. *Sustainable Cities and Society, 126*, Article 106384.

Wilson, M. H., Habig, K., Wright, C., Hughes, A., Davies, G., & Imray, C. H. (2015). Pre-hospital emergency medicine. *The Lancet, 386*(10012), 2526–2534.

World Health Organization. (2024). *Aging and health*. https://www.who.int/news-room/fact-sheets/detail/ageing-and-health.

Xu, N., Bai, J., & Yan, R. (2022). Identifying the vulnerable regions of emergency medical services based on the three-stage of accessibility: A case study in Xi'an, China. *International Journal for Equity in Health, 21*(1), 54.

Yan, H., Pan, S., Zhang, S., Wu, F., & Hao, M. (2024). Sustainable utilization of road assets concerning obscured traffic signs recognition. In *, 178. Proceedings of the Institution of Civil Engineers-Engineering Sustainability* (pp. 124–134).

Yang, Z., Guo, Y., Feng, X., Zhou, Y., Zhou, P., Li, X., & Qian, X. (2024). Evaluating temporal variations in access to multi-tier hospitals using personal vehicles and public transit: Implications for healthcare equity. *Sustainable Cities and Society, 113*, Article 105687.

Ye, X., Li, S., Gong, W., Li, X., Li, X., Dadashova, B., … Wu, D. (2025). Street view imagery in traffic crash and road safety analysis: A review. *Applied Spatial Analysis and Policy, 18*(2), 50.

Zhang, E., Hsu, W., Long, Y., & Hawken, S. (2023). *Understanding bikeability: Insight into the cycling-city relationship using massive dockless bike-sharing records in Beijing*. Paper presented at the Intelligence for Future Cities, Cham.

Zhang, F., Salazar-Miranda, A., Duarte, F., Vale, L., Hack, G., Chen, M., … Ratti, C. (2024a). Urban visual intelligence: Studying cities with artificial intelligence and street-level imagery. *Annals of the American Association of Geographers, 114*(5), 876–897.

Zhang, S., Wang, L., Shen, Y., Zhang, Y., Gao, Y., Xu, T., & Zhang, Z. (2024b). What causes emergency medical services (EMS) delay? Unravel high-risk buildings using citywide ambulance trajectory data. *Habitat International, 153*, Article 103198.

Zhu, H., Pan, L., Li, Y., Jin, H., Wang, Q., Liu, X., … Li, L. (2021). Spatial accessibility assessment of prehospital EMS with a focus on the elderly population: A case study in Ningbo, China. *International Journal of Environmental Research and Public Health, 18*(19), 9964.